FT-IR Study of Water Adsorption on Aluminum Oxide Surfaces

Hind A. Al-Abadleh and V. H. Grassian*

Departments of Chemistry and Chemical and Biochemical Engineering, University of Iowa, Iowa City, Iowa 52242

Received July 9, 2002. In Final Form: October 18, 2002

In this study, transmission FT-IR spectroscopy is used to investigate the adsorption of water on aluminum oxide surfaces, including both single-crystal and particle surfaces. The FT-IR spectra of the (0001) surface of α-Al_2O_3 single crystals at 296 K in the presence of 0.2 to 20 Torr H_2O vapor pressure corresponding to 1 to 95% relative humidity (RH) have been measured. The FT-IR spectra are shown to change as a function of RH. At low relative humidity, below approximately 10%, water adsorbs on the surface in an ordered fashion with the formation of a stable hydroxide layer. At intermediate RH, between 10 and 70% RH, water adsorbs molecularly in a structured overlayer. At high RH, greater than 70%, water adsorption is more disordered and consistent with the formation of a liquid-like water layer. The adsorption of nitric acid on α-Al_2O_3(0001) prior to water adsorption is shown to only slightly modify the water infrared spectra. A discussion of the quantification of the number of water layers on the α-Al_2O_3(0001) surface as a function of RH as well as a comparison of water adsorption on single-crystal α-Al_2O_3(0001) to that on α- and γ-Al_2O_3 powders are presented here.

Introduction

Aerosols are emitted into the troposphere from different sources. The largest contribution to tropospheric aerosols is from mineral dust that is produced mainly from wind-blown soils.[1] Mineral dust aerosols are composed in part of silicate minerals and clays as well as other oxides such as α-Al_2O_3 (corundum) and hematite (α-Fe_2O_3).[2] The amount of mineral dust emitted into the atmosphere is estimated to be between 1000 and 3000 Tg per year.[1] Under certain atmospheric conditions of temperature, pressure, and relative humidity, some of these aerosol particles can serve as cloud or ice condensation nuclei, depending on the chemical composition of the aerosols and their solubility in water. Lattice matching between the surface structure of the aerosol and that of ice can also enhance ice formation, even at relatively high temperatures.[1] It has also been recently reported[2] that adsorbed water enhances the uptake of trace atmospheric gases such as nitric acid on α-Al_2O_3. Thus, water adsorption on minerals is of extreme interest.[3−6]

The focus of this study is on the adsorption of water on Al_2O_3 surfaces. Besides its potential role in acting as an ice condensation nucleus,[4] there is a great deal of interest in the uptake of water on Al_2O_3 surfaces as aluminum oxides are widely used as catalysts and catalyst supports. Aluminum oxides are also used as structural ceramic materials, and aluminum alloys and their oxides are of great interest in the automobile industry. Water uptake on the surfaces of these technologically important interfaces can affect their reactivity and performance.[3,7,8]

There have been several studies on the uptake of water on alumina powders. In one study, immersion calorimetry was used to measure the heat of adsorption of water on α- and γ-alumina powders that have been outgassed at temperatures of 600 °C.[9] This study showed that the heat of adsorption on γ-Al_2O_3 is higher than on α-Al_2O_3 at corresponding water coverages. It was also found that the degree of surface dehydration prior to water adsorption could affect the value of the heat of adsorption. In another study using X-ray diffraction and Raman and infrared spectroscopy at room temperature, Dyer et al.[10] looked at the hydration of the γ-Al_2O_3 surface. The XRD data showed the formation of $Al(OH)_3$ in the bayerite polymorph which disappeared after heating to 200 °C. The IR spectra of γ-Al_2O_3 powder show several sharp but weak features after hydration in the region around 3600 cm^{-1}.

Water uptake on α- and γ-Al_2O_3 powder as a function of relative humidity at 296 K has been studied in our laboratory.[2] Water adsorption on these oxides was modeled using a modified BET analysis in order to quantify the number of adsorbed water layers. For α-Al_2O_3, a complete monolayer of water is calculated to occur around 17% RH. However, it was noted in that work that there are complications associated with studies of porous powders that make interpretation of the data difficult. For example, powder samples have different crystallographic orientations compared to single crystals of well-defined crystallographic planes. Thus, the dependence of water adsorption and surface hydroxylation on the surface orientation will be difficult if not impossible to interpret using powder samples compared to single crystals.[11] One of the difficulties associated with adsorption and desorption kinetics on porous materials is that the distinction between

* Author to whom correspondence should be addressed.

(1) Seinfeld, J. H.; Pandis, S. N. *Atmospheric Chemistry and Physics*; John Wiley & Sons: New York, 1997.
(2) Goodman, A. L.; Bernard, E. T.; Grassian, V. H. *J. Phys. Chem. A* **2001**, *105*, 6443.
(3) Eng, P. J.; Trainor, T. P.; Brown, G. E., Jr.; Waychunas, G. A.; Newville, M.; Sutton, S. R.; Rivers, M. L. *Science* **2000**, *288*, 1029.
(4) Cantrell, W.; Ewing, G. E. *J. Phys. Chem. B* **2001**, *105*, 5434.
(5) Zuberi, B.; Bertram, A. K.; Koop, T.; Molina, L. T.; Molina, M. J. *J. Phys. Chem. A* **2001**, *105*, 6458.
(6) Zuberi, B.; Bertram, A. K.; Cassa, C. A.; Molina, L. T.; Molina, M. J. *Geophys. Res. Lett.* **2002**, *29*, 142/1.
(7) Elam, J. W.; Nelson, C. E.; Cameron, M. A.; Tolbert, M. A.; George, S. M. *J. Phys. Chem. B* **1998**, *102*, 7008.
(8) Hass, K. C.; Schneider, W. F.; Curioni, A.; Andreoni, W. *J. Phys. Chem. B* **2000**, *104*, 5527 and references therein.
(9) Hendriksen, B. A.; Pearce, D. R.; Rudham, R. *J. Catal.* **1972**, *24*, 82.
(10) Dyer, C.; Hendra, P. J.; Forsling, W.; Ranheimer, M. *Spectrochim. Acta* **1993**, *49A*, 691.
(11) Liu, P.; Kendelewicz, T.; Brown, G. E., Jr.; Nelson, E. J.; Chambers, S. A. *Surf. Sci.* **1998**, *417*, 53.

10.1021/la026208a CCC: $25.00
Published on Web 12/21/2002

condensation and adsorption of the first monolayer is often elusive.[12] Capillary condensation into micropores, flux of adsorbates arriving to the surface, and transport kinetics of adsorbates through the pores are all factors that will complicate the measurement of fundamental surface processes.[13]

The adsorption of water on single-crystal α-Al_2O_3(0001) surfaces has been studied with several techniques under ultrahigh vacuum (UHV) conditions using laser-induced thermal desorption (LITD) and temperature-programmed desorption (TPD).[7] Although a rather high initial sticking coefficient of 0.1 has been measured for H_2O on α-Al_2O_3(0001) at 300 K, it was found that the sticking coefficient decreases exponentially with coverage. In another study,[11] the reaction of water vapor on α-Al_2O_3(0001) was investigated at higher pressures using synchrotron X-ray photoemission spectroscopy. It was shown that hydroxylation occurred at a vapor pressure of water comparable with the calculated threshold pressure for the conversion of corundum to gibbsite, $Al(OH)_3$, according to reaction 1.[7]

$$Al_2O_3 + 3H_2O \rightarrow 2Al(OH)_3 \qquad (1)$$

This is in accordance with the molecular dynamics study by Hass et al.[14] that shows a negligible energy barrier for water dissociation at room temperature.

In a more recent study,[3] the structure of the hydrated α-Al_2O_3(0001) surface has been investigated in the presence of water vapor at 300 K by crystal truncation rod diffraction using a synchrotron X-ray source. The results indicated that the hydrated alumina surface is oxygen terminated and that the structure is actually an intermediate between α-Al_2O_3 and γ-$Al(OH)_3$ with the surface terminated by a monolayer of OH under ambient conditions. Water can then molecularly adsorb in a partly ordered overlayer on top of the OH-terminated surface.

In this study, transmission Fourier transform infrared (FT-IR) spectroscopy is used to investigate the adsorption of water on the α-Al_2O_3(0001) surface at room temperature and in the presence of 0.2 to 20 Torr H_2O vapor pressure. The FT-IR data of water adsorbed on α-Al_2O_3(0001) presented here are analyzed to obtain structural information about the partially ordered overlayer and to quantify the number of water layers on the surface as a function of relative humidity. Water adsorption on α-Al_2O_3(0001) surfaces that have been exposed to nitric acid are also investigated in order to determine how adsorbed ions can affect the hydrogen-bonding network of the adsorbed water overlayer. Finally, a comparison between the single-crystal data and that of water adsorption on α- and γ-Al_2O_3 powders is also discussed.

Experimental Section

Spectroscopic measurements were done using an FT-IR spectrometer (Mattson RS-1) equipped with a liquid nitrogen cooled narrow band MCT detector. Spectra of gas-phase water and α-Al_2O_3(0001) single crystals before and after the introduction of water were acquired by averaging 1000 scans at a resolution of 8 cm^{-1} in the region extending from 750 to 5000 cm^{-1}. The water source was obtained from Optima water (Fisher Scientific, Optima water) and was subjected to several cycles of freeze−pump−thaw before use. For D_2O experiments, a sample was prepared by transferring some D_2O (Alfa Aesar deuterium oxide 99.8%) to a 100 mL glass flask under a nitrogen atmosphere. The D_2O sample was subjected to several cycles of freeze−pump−thaw before use as well. Dry gaseous nitric acid was taken from the vapor of a 1:3 by volume mixture of concentrated HNO_3 (70.6% HNO_3, Mallinckrodt) and H_2SO_4 (95.9%, H_2SO_4, Mallinckrodt).

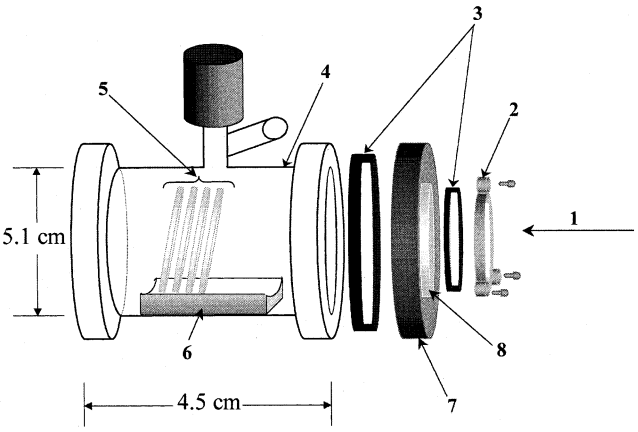

Figure 1. Schematic of the glass infrared cell used to study the adsorption of water on single-crystal surfaces: 1. direction of incident light; 2. aluminum holder for Ge windows; 3. O-rings; 4. Pyrex glass infrared cell of volume, V ($V = 122 \pm 4$ mL); 5. α-Al_2O_3(0001) single crystals, spacing between crystals was 2 mm; 6. Teflon-holder for single crystals; 7. stainless steel holder for Ge windows; 8. Ge window.

An infrared cell and gas handling system were specially designed for these studies and is a slightly modified version of the design described by Ewing and co-workers.[15] The gas handling system consists of a four-port glass manifold that is connected to two absolute pressure transducers (MKS instruments) that operate in the range from 0.001 to 10.00 Torr and 0.1 to 1000 Torr. The gas manifold is connected to an Alcatel turbo molecular pump (140 L/s, rough pumped with a mechanical Leybold D4A, 127 L/min). The volume of the glass manifold is 662 ± 3 mL. The gas handling system is connected to the IR cell through a Teflon tube. A cylindrical 4.5×5.1 cm Pyrex IR cell (volume $= 122 \pm 4$ mL) was placed in the spectrometer sample compartment (see Figure 1). Two wedged Ge windows (Janos Technology Inc.) were placed in two stainless steel holders that are O-ring sealed to the Pyrex IR cell. A Teflon holder placed inside the infrared cell held the single crystals in place.

The α-Al_2O_3(0001) single crystals were purchased from MTI Corporation. A total of twelve 0.5 mm thick single crystals were polished on both sides. The single crystals were placed on a Teflon holder inside the IR cell and canted 45° with respect to vertical to minimize the effects of Etalon fringes.[4]

The single crystals were calcined in air at 873 K for overnight before use. This procedure ensures the removal of adsorbed carbonaceous species as indicated by Auger electron spectroscopy (AES). Other cleaning procedures were also tried, such as etching with dilute HNO_3 solution, but found unsatisfactory and inefficient in removing residual carbon as shown by AES analysis. Crystals were kept in an oven at 413 K between experiments intended to reproduce results and were directly placed in the IR cell to cool under vacuum. Background scans of the single crystals were recorded before introducing water. Water was introduced into the infrared cell and allowed to equilibrate for at least 20 min before each spectrum was recorded. All spectra were recorded in the presence of gas-phase water as a function of water vapor pressure (0.2 to 20 Torr) at 296 K, corresponding to 1 to 95% RH. Even though the infrared cell was designed such that gas-phase water absorptions were minimized, it was still necessary to subtract water absorptions from all of the spectra shown for water adsorption on α-Al_2O_3(0001).

Water adsorption on α-Al_2O_3 (Alfa Aesar) and γ-Al_2O_3 (Degussa) powders was also investigated at ambient temperatures and as a function of water vapor pressure. BET surface areas of these powders were determined using a Quantachrome

(12) Sneh, O.; Cameron, M. A.; George, S. M. *Surf. Sci.* **1996**, *364*, 61.

(13) Gregg, S. T.; Sing, K. S. W. *Adsorption, Surface area and Porosity*; Academic Press: NewYork, 1982.

(14) Hass, K. C.; Schneider, W. F.; Curioni, A.; Andreoni, W. *Science* **1998**, *282*, 265.

(15) Foster, M. C.; Ewing, G. E. *J. Chem. Phys.* **2000**, *112*, 6817.

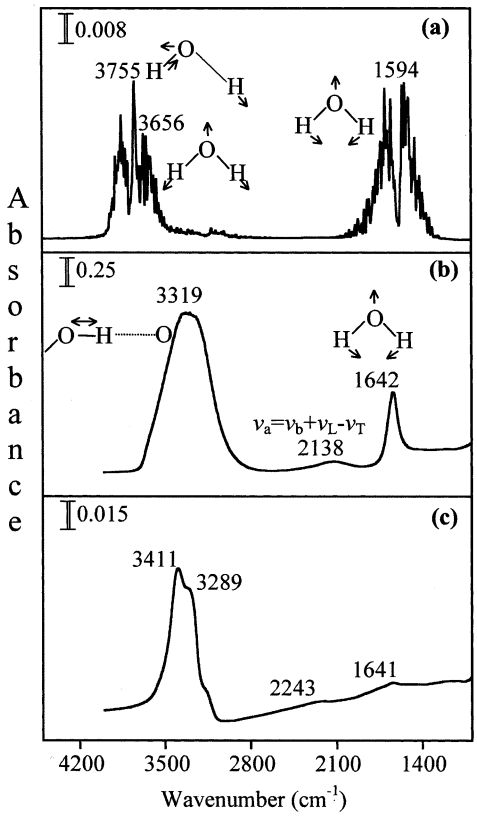

Figure 2. FT-IR spectra of water in the (a) gas, (b) liquid, and (c) solid phase.

Nova 1200 multipoint BET apparatus and were found to be 8.1 and 101 m^2/g for α-Al_2O_3 and γ-Al_2O_3, respectively. The average particle diameter was measured using a Hitachi H-6000 transmission electron microscope and found to be 400 and 18 nm for α-Al_2O_3 and γ-Al_2O_3, respectively.

For the FT-IR measurements, oxide particles were coated onto half of a tungsten grid (3 cm × 2 cm, 100 mesh/in., 0.002″ wire dia., Accumet Materials Co.).The grid is then mounted inside an IR cell that has been described previously.[2] The IR cell consists of a stainless steel cube placed on a linear translator inside the internal compartment of the FT-IR spectrometer. The linear translator allows each half of the sample grid to be placed in the IR beam path in order to acquire spectra of the blank side which contains absorptions due to gas-phase molecules and the oxide-coated side which contains absorptions due to adsorbed and gas-phase molecules. FT-IR spectra of both halves were acquired in the presence of gas-phase water by averaging 250 scans at 4 cm^{-1} resolution in the spectral range extending from 750 to 4000 cm^{-1}. Gas-phase absorptions were then subtracted from the adsorbate spectra.

Results and Discussion

1. Infrared Spectroscopy of Water in the Gas, Liquid, and Solid Phases. Effect of Hydrogen Bonding on the Vibrational Modes of Water. Figure 2 shows infrared spectra of water in three phases: (a) gas, (b) liquid, and (c) solid. The isolated water molecule has three normal modes of vibration. In the gas phase, the symmetric and asymmetric OH stretching vibrations (ν_1, ν_3) have band centers at 3656 and 3755 cm^{-1} and the bending mode, $\delta(H_2O)$, has a band center at 1594 cm^{-1}.[16] Upon formation of hydrogen bonds in the liquid phase and because of the broadening of the spectral features, there is no distinction between ν_1 and ν_3. Instead, the hydrogen-bonded OH stretch will collapse to a diffuse absorption band that is red-shifted 200−400 cm^{-1} from the gas-phase values. Moreover, the full width at half-maximum (fwhm) of the ν(OH) will broaden as a result of hydrogen bonding and will show a dependence on the heterogeneity of the molecular environment of hydrogen-bonded water molecules. In general, the more disordered the molecular environment, the broader the band.[17,18] Therefore, the OH region in the liquid water spectrum is broader than that found in the ice spectrum. Besides the red shift in the OH stretching frequencies, formation of hydrogen bonds between water molecules is also accompanied by an increase in the integrated cross section.[19]

The bending mode region of different solid phases of water has been extensively studied by Devlin and Coworkers.[20,21] The bending mode shifts upward upon formation of hydrogen bonds.[19] It is apparent in the infrared absorbance spectra of liquid water and microporous amorphous ice at 1645 and 1670 cm^{-1}, respectively.[20]

Frustrated rotations (libration modes) and frustrated translations are other vibrational modes of condensed-phase water. Frustrated rotations are observed in the mid-IR region at 685 cm^{-1} for liquid water and at 830 cm^{-1} for ice.[22,23] The librational modes are known to shift upward in frequency upon hydrogen bonding accompanied by an increase in intensity and bandwidth.[19] In addition, the intensity of the bending mode decreases and its overlap with the overtone of the librational mode increases as the strength and/or the number of hydrogen bonds to water molecules increases.

Absorptions are observed around 2200 cm^{-1} for both liquid water different phases of ice. For liquid water, the broad feature is centered at 2100 $cm^{-1}$and assigned to an association band (ν_a) which is a combination of the bending, δ, libration, ν_L, and hindered translation, ν_T, modes.[24] However, the band observed in this region for different phases of ice is centered around 2255 cm^{-1} and has been recently reassigned to the second overtone frequency of the librational fundamental.[20]

2. FT-IR Spectra and Analysis of Water and Deuterated Water Adsorbed on the (0001) Surface of α-Al_2O_3 at 296 K. Representative spectra obtained of the α-Al_2O_3(0001) surface at 296 K as a function of water vapor pressure are shown in Figures 3 and 4. The spectra are recorded as a function of increasing relative humidity in the presence of water vapor. A series of gas-phase water spectra at different pressures were measured and used to subtract out the gas-phase absorptions from the spectra shown in Figures 3 and 4. The subtraction process can cause anomalous absorption errors. A complete investigation of this problem and ways to circumvent it have been discussed in detail by Weis and Ewing.[25]

The low RH and low coverage spectra are shown in Figure 3. The spectra show two broad absorptions of approximately equal intensity with frequencies of 3430 and 3280 cm^{-1}. A shoulder at higher frequencies, near 3547 cm^{-1}, is often apparent in spectra at low RH but has

(16) Eisenberg, D.; Kauzmann, W. *The Structure and Properties of Water*; Oxford University Press: New York and Oxford, 1969.

(17) Jeffrey, G. A. *An Introduction to Hydrogen Bonding*; Oxford University Press: New York, 1997.

(18) Thiel, P. A.; Madey, T. E. *Surf. Sci. Rep.* **1987**, *7*, 211.

(19) Pimentel, G. C.; McClellan, A. L. *The Hydrogen Bond*; W. H. Freeman and Co.: San Francisco and London, 1960.

(20) Devlin, J. P.; Sadlej, J.; Buch, V. *J. Phys. Chem. A* **2001**, *105*, 974.

(21) Hernandez, J.; Uras, N.; Devlin, J. P. *J. Chem. Phys.* **1998**, *108*, 4525.

(22) Oder, R.; Goring, D. A. I. *Spectrochim. Acta* **1971**, *27A*, 2285.

(23) Ikawa, S. I.; Maeda, S. *Spectrochim. Acta* **1968**, *24A*, 655.

(24) Williams, D. *Nature* **1966**, *210*, 194.

(25) Weis, D. D.; Ewing, G. E. *Anal. Chem.* **1998**, *70*, 3175.

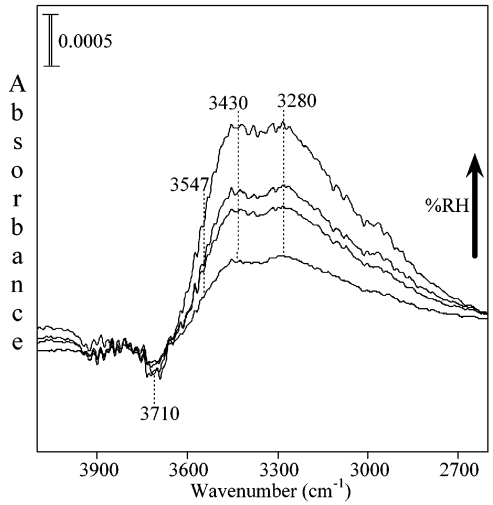

Figure 3. Representative transmission FT-IR spectra for low coverage water adsorption on the α-Al_2O_3(0001) surface at 296 K as a function of relative humidity, 0.6, 1.6, 2.9, 6.2%.

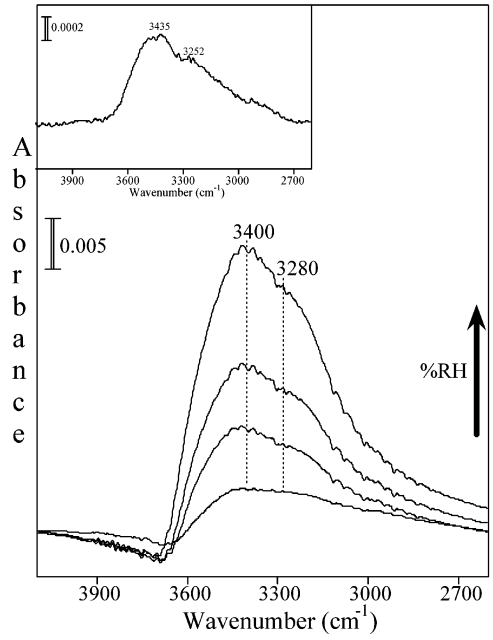

Figure 4. Representative transmission FT-IR spectra for water adsorption on the α-Al_2O_3(0001) surface at 296 K as a function of relative humidity, 16, 47, 73, 90%. Inset: surface-bound species after evacuation of gas-phase water.

variable intensity and is found to depend on the exact pretreatment of the α-Al_2O_3(0001) surface. Surfaces calcined in air to 873 K do not show an obvious shoulder compared to surfaces calcined at lower temperatures. This peak may be related to impurities present on the surface such as the presence of adventitious carbon-containing impurities as has been discussed previously by others.[3] Similar experiments at low RH with deuterated water show absorptions at 2527 and 2407 cm^{-1} with a high-frequency shoulder at 2632 cm^{-1} when carbon is present.

As RH increases and the coverage of adsorbed water increases, the spectral features noted above increase in intensity up to ~10% RH where at that point there is a change in intensity and band shape (see Figure 4). There is a large increase in the intensity in the region extending from 3400 to 3600 cm^{-1} at that point. The infrared spectra in the intermediate RH range (10−70% RH) begin to look similar to the ice spectrum shown in Figure 2. At the

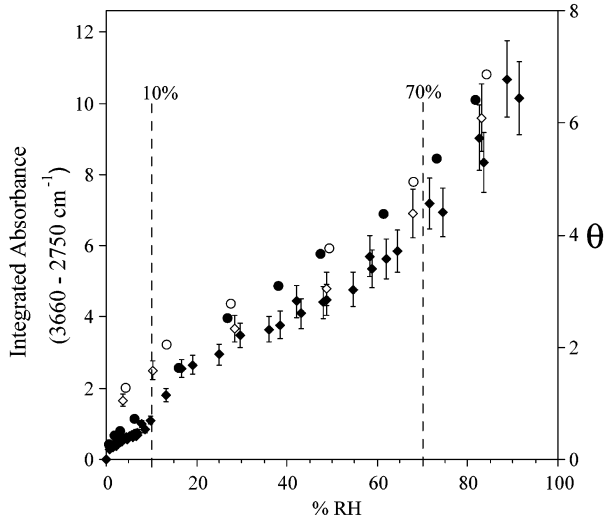

Figure 5. Integrated absorbance of the OH region (*y*-left axis) plotted as a function of relative humidity. Filled circles and diamonds are increasing water vapor pressure. Open circles and diamonds are for decreasing water vapor pressure. Two different data sets are shown. Error bars are only shown for one of the data sets. Circles are for water adsorbed on calcined α-Al_2O_3(0001), and diamonds are for water adsorption on α-Al_2O_3(0001) exposed previously to water and stored in an oven at 413 K for 24 h. The integrated absorbance is converted to a coverage theta, θ (*y*-right axis), as defined in eq 5. The dotted line marks the different regions observed in the infrared data, see text for further discussion.

highest RH, at 90% RH, there is a broad absorption band with a band center at 3400 cm^{-1}. A difference spectrum of the 73 and 90% RH data reveal that at the highest water coverages a broad absorption near 3400 cm^{-1} grows on top of the structured absorption seen in the spectra recorded at the intermediate RH range.

Upon evacuation of gas-phase water from the infrared cell, there are two weak but distinct bands present at 3435 and 3252 cm^{-1}, as seen in the inset of Figure 4. These bands are present even after overnight evacuation. It should also be noted that there is also a slight loss in absorption around 3710 cm^{-1} in the water spectrum. This may signify the presence of isolated hydroxyl groups before the start of the experiment that become hydrogen-bonded to molecular water.[8]

Figure 5 shows the integrated area of the OH band in the range extending from 3660 to 2750 cm^{-1} plotted as a function of increasing and decreasing relative humidity. The large error bars given for %RH > 90 are because of a small temperature gradient between the water source and the IR reaction cell. This temperature difference causes condensation of water vapor pressure on the walls of the glass manifold, especially when water vapor pressure approaches its saturation pressure at 296 K which is 21.08 Torr. Two data sets are shown in Figure 5. For clarity, error bars are shown only for one of the data sets. The first is for surfaces calcined in air at 873 K and the second is for surfaces calcined in air at 873 K and then stored at 413 K for 24 h. The data shown in Figure 5 are for both increasing (filled symbols) and decreasing (open symbols) water vapor pressure. Note there is a hysteresis observed in the adsorption/desorption data (i.e., increasing/decreasing water vapor pressure data) below 10% RH.

To quantify the integrated absorbance in terms of water surface coverage, so that an adsorption isotherm for water on the (0001) surface of the α-Al_2O_3 single crystals at 296 K can be obtained, we start with a modified form of Beer−

Lambert's law that has been used to determine the extent of water coverage on mica:[4]

$$\tilde{A} = \int_{\text{band}} A \, d\nu = \frac{N\rho \, l}{2.303 \cos \phi} \cdot \int_{\text{band}} \sigma \, d\nu \qquad (2)$$

where $\tilde{A}$ is the integrated absorbance (cm^{-1}), N is the number of adsorption surface faces (24 in these experiments), ρ is the molecular density of water (for liquid water, $\rho = 3.35 \times 10^{22}$ molecule cm^{-3} at 296 K), l is the thickness of the adsorbed layer (cm), σ is the frequency-dependent cross section of liquid water (cm^2/molecule), and ϕ is the angle of incidence. This equation can be written as

$$\tilde{A} = \frac{N S_{H_2O} \bar{\sigma}}{2.303 \cos \phi} \qquad (3)$$

where S_{H_2O} is equal to the surface density of adsorbed water in units of molecules cm^{-2} ($S_{H_2O} = \rho l$) and

$$\bar{\sigma} = \frac{4\pi}{\rho} \int_{\text{band}} \kappa \tilde{\nu} \, d\tilde{\nu} \qquad (4)$$

where κ is the wavenumber-dependent extinction coefficient integrated over the OH band (3660−2750 cm^{-1}). Using the values of κ for liquid water[26] leads to a value of $\bar{\sigma}$ of 1.07×10^{-16} cm $molecule^{-1}$.

Equation 3 can be used to convert the integrated absorbance to surface density of adsorbed water, S_{H_2O}. The number of adsorbed water layers can be calculated by

$$\theta = \frac{S_{H_2O}}{S_{(0001)}} \qquad (5)$$

where $S_{(0001)}$ is the density of the OH-terminated (0001) surface of α-Al_2O_3. For complete OH termination, $S_{(0001)}$ is calculated to be 1.5×10^{15} OH cm^{-2}. However, under the conditions of our experiments, the α-Al_2O_3(0001) will have some degree of OH termination as is evident by the negative band at 3710 cm^{-1}. In fact, more than one study has shown that it is difficult to completely remove hydroxyl groups, even by thermal treatment.[27,28] The only way for the complete removal of hydroxyl groups is by sputtering and annealing in UHV as found by Niu et al.[29] In addition, diffraction studies show that the OH-terminated α-Al_2O_3(0001) surface is intermediate between α-Al_2O_3 and γ-$Al(OH)_3$.[3] Thus, a value of 1×10^{15} for $S_{(0001)}$ may be more likely.[7] Using this value for $S_{(0001)}$, a coverage of one monolayer is seen to occur near 10% RH.

It is important to note that there are uncertainties associated with the calculation of surface coverage using the modified Beer−Lambert's law. These uncertainties have been addressed previously.[4,30] Briefly, errors arise principally from three parameters, $\bar{\sigma}$ (the integrated cross section), ρ (molecular density of the adsorbed water layer), and $S_{(0001)}$ (the OH surface density). The integrated cross section (or the oscillator strength) changes as a function of water coverage due to changes in the hydrogen-bonding network. Thus, using the parameters of liquid water in calculating $\bar{\sigma}$ will cause an uncertainty, especially in the low-coverage region where strongly adsorbed water clusters can exist as well as hydroxyl groups. That uncertainty in $\bar{\sigma}$ at low coverage (which is expected to be higher than the value for the liquid water, $\bar{\sigma} = 2.05 \times 10^{-16}$ and 6.38×10^{-16} cm/molecule calculated for the asymmetric and symmetric stretch of D_{2d} water octamers, respectively[31]) is compensated by a decrease in the molecular density of water as liquid becomes ice. If we wanted to quantify this compensation, we can say that $\bar{\sigma}$ for ice is greater than that for liquid by approximately a factor of 2 in the OH stretch region.[15] The density of amorphous ice Ih is 0.93 g/cm^3 at 163 K[32] which differs by only 0.07 g/cm^3 from that of liquid, 1 g/cm^3 at RT. Since density is temperature dependent, the compensation of the increase in $\bar{\sigma}$ and decrease in ρ will not be completely canceled out. Two other factors that cause uncertainty in our θ calculations is the value of $S_{(0001)}$ which we estimate to be near 1×10^{15} OH cm^{-2} and the fact that dissociation of water to yield a layer of hydroxyl groups is most likely occurring at low relative humidity as well (vide infra).

Another method to predict at which %RH a molecular layer of liquid water will form on α-Al_2O_3 is through the use of eq 3. If the molecular density of liquid water at 296 K and an average thickness of 310 pm are assumed,[30] the integrated absorbance, $\tilde{A}$, for one layer of water can be calculated. From this, a value of 1.6 for absorbance units corresponds to one monolayer of adsorbed water and that occurs at ∼10% RH.

It should be also noted that the adsorption data presented in Figure 5 exhibits an s-shaped-like isotherm curve, which indicates mulitlayer formation. Since single-crystal surfaces are considered to be uniform surfaces on which an infinite number of layers form when the pressure of the gas approaches the saturation vapor pressure, our data can be fit to a two-parameter Type II BET fit, which has the linear form:[33]

$$\frac{x}{(1-x)V} = \frac{1}{V_m c} + \frac{(c-1)}{V_m c} x, \qquad x = \frac{P}{P_o} \qquad (6)$$

where V is the volume of gas adsorbed at equilibrium pressure P, V_m is the volume of gas necessary to complete a monolayer, P_o is the saturation vapor pressure of the adsorbing gas at that temperature, and c is the temperature-dependent constant related to the enthalpies of adsorption of the first layer and higher layers as in eq 7:

$$c = \exp - \left[\frac{\Delta H_1^\circ - \Delta H_2^\circ}{RT} \right] \qquad (7)$$

where ΔH_1° is the standard enthalpy of adsorption of the first layer, and ΔH_2° is the standard enthalpy of adsorption of subsequent layers and is taken as the enthalpy of condensation of water vapor, which is equal to −44.0 kJ/mol.

Figure 6 shows that the BET isotherm data of water adsorption on the (0001) surface of the alumina single crystals is not linear in the RH range under investigation. The surface coverage of water molecules, S_{H_2O}, is used instead of the volume of the adsorbed gas, V, in eq 6. Two discontinuities occur near $x = 0.1$ and 0.7, corresponding to 10 and 70% RH, that appear to form three regimes of different slopes. The BET model assumes energetically equivalent adsorption sites.[13] The model does not take

(26) Downing, H. D.; Williams, D. J. *J. Geophys. Res.* **1975**, *80*, 1656.
(27) Ahn, J.; Rabalais, J. W. *Surf. Sci.* **1997**, *388*, 121.
(28) Kelber, J. A.; Niu, C.; Shepherd, K.; Jennison, D. R.; Bogicevic, A. *Surf. Sci.* **2000**, *446*, 76.
(29) Niu, C.; Shepherd, K.; Martini, D.; Tong, J.; Kelber, J. A.; Jennison, D. R.; Bogicevic, A. *Surf. Sci.* **2000**, *465*, 163.
(30) Sadtchenko, V.; Conrad, P.; Ewing, G. E. *J. Chem. Phys.* **2002**, *116*, 4293.
(31) Estrin, D. A.; Paglieri, L.; Corongiu, G.; Clementi, E. *J. Phys. Chem.* **1996**, *100*, 8701.
(32) *CRC Handbook Of Chemistry and Physics*, 72nd ed.; CRC Press: Boca Raton, FL, 1991.
(33) Atkins, P. *Physical Chemistry*, 6th ed.; Freeman: NewYork, 1997.

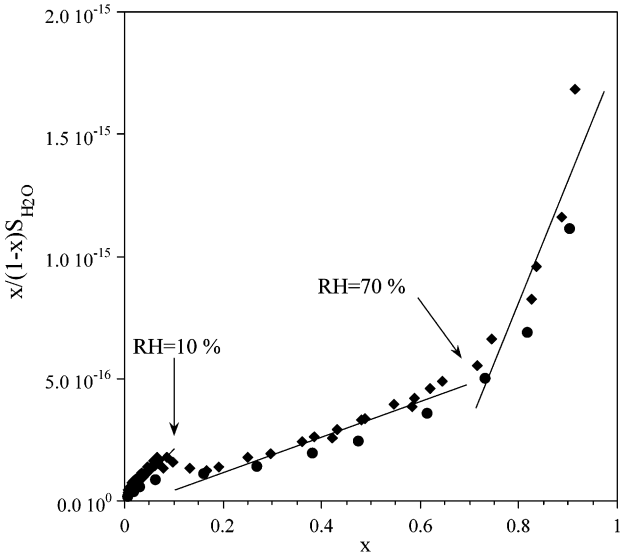

Figure 6. The linear form of the BET model, eq 6, for the isotherm data of water adsorption on the (0001) surface of α-Al_2O_3 using the adsorption data presented in Figure 5.

into account interactions between adosrbate molecules and therefore does not adequately describe water adsorption on surfaces.

Although the BET equation is inadequate in the analysis of the water adsorption isotherm, the linearized BET equation defines the three regions that are observed in the FT-IR spectra. Region I occurs below 10% RH, Region II characterizes the spectra recorded from 10 to 70% RH, and Region III represents spectra recorded above 70% RH. The structure of the water layer defined by these three regions can be discussed in light of the previous studies on water adsorption on α-Al_2O_3(0001) using other surface analysis methods and FT-IR studies of other single-crystal surfaces.

As noted by by Liu and co-workers[11] in their studies using XPS, at low RH α-Al_2O_3(0001) converts to $Al(OH)_3$ and the crystal-rod diffraction study of Eng et al.[3] also indicates the presence of a hydroxide layer. Below 10% RH, the infrared data are consistent with the formation of a hydroxide layer that is hydrogen-bonded to molecular water as evidenced by its low frequencies.[34] The formation of a hydroxide layer may involve a cooperative effect that is assisted by intact, hydrogen-bonded water molecules.[35] A hysteresis is also observed below 10% in the adsorption/desorption data shown in Figure 5. This hysteresis is consistent with the formation of a hydroxlated layer upon adsorption at low relative humidity. In the intermediate coverage range between 10 and 70% RH, the FT-IR data with bands at 3400 and 3280 cm^{-1} are similar to the ice spectra shown in Figure 2. This is again consistent with the crystal-rod truncation data of Eng et al.[3] where a structured molecular water layer was seen at 50% RH. In the high coverage range, which occurs above 70% RH, the infrared difference spectra indicate that a more disordered layer forms on top of the structured layer.

Water adsorption on mica surfaces has been studied to differentiate between wetting and clustering of water since no alteration of surface properties upon high-pressure water adsorption can occur on these relatively inert materials.[36] Muscovite mica has the chemical formula of $KAl_2[AlSi_3]O_{10}(OH)_2$. As discussed by Cattrell and Ewing,[4] the adsorption of water on mica at room temperature also shows three chemically and spectroscopically distinct coverage regimes: high ($\theta = 2.5$), monolayer ($\theta = 1$), and low ($\theta = 0.5$). At the submonolayer coverage, the FT-IR spectrum shows an asymmetric OH band with maximum absorption near 3350 cm^{-1}, tailing off toward 2700 cm^{-1}, and absorption features between 3300 and 3000 cm^{-1}. It is difficult to see water absorptions in the range 3500−3700 cm^{-1} because of strong absorptions due to the mica substrate. The absorptions in the 3300−3000 cm^{-1} were in accord with the vibrational modes calculated for hexamers and higher-order clusters and with molecular dynamics calculations (MD) for the structure of a monolayer on the mica surface. The MD calculations indicate that the structure of a monolayer is puckered hexagons of water locked to an underlying mica substrate. Other studies of water on mica show that these films exhibit surface-induced ferrolelectric ice behavior.[37] The higher coverage monolayer and multilayer spectra ($\theta \geq 1$) of water on mica were reported to be more of a liquid-like rather than an ice-like bilayer. These results indicate that, at high water coverage, water molecules are hydrogen-bonded to each other and not necessarily occupying all sites on the mica surface.

Water adsorption on the BaF_2(111) surface[30] shows a diffuse doublet with one component centered at 3460 cm^{-1} and shifted to 3400 cm^{-1} at high water coverage. This doublet signature indicates a well-structured, ice-like adlayer that forms on the BaF_2(111) surface, even at room temperature. Again at high water coverage, the infrared spectra showed evidence for a liquid-like water film.

3. FT-IR Spectra of Water Adsorbed on α-Al_2O_3 at 296 K after Adsorption of Nitric Acid. Adsorption of HNO_3 on α-Al_2O_3(0001) single crystals was carried out at 296 K. Only changes in the spectral range extending 1600 to 4000 cm^{-1} were analyzed due to the strong absorptions of the alumina single crystals below 1600 cm^{-1} that make it difficult to analyze that low-frequency region. In these experiments, eleven crystals were allowed to react with gas-phase HNO_3 as a function of pressure (65, 129, 223, 286, and 466 mTorr) for 20 min each. Spectra were recorded in the presence of gas-phase HNO_3 and after evacuation of the corresponding pressure. The surface was reacted with the mixture of gas-phase H_2O and HNO_3 for thirty minutes as it has been shown in previous studies that water enhances the adsorption uptake kinetics for nitric acid on aluminum oxide powders.[2] Following exposure to nitric acid, the crystals were exposed to water vapor as a function of RH.

Transmission FT-IR spectra of water adsorbed on these α-Al_2O_3(0001) surfaces that have been reacted with HNO_3 at 296 K as a function of increasing relative humidity was investigated. No obvious changes were observed in the infrared spectra of adsorbed water on these surfaces compared to the clean surfaces. This is in contrast to the large differences found for water adsorption on nitric acid reacted MgO(100) compared to unreacted MgO(100).[38] Difference spectra taken between water adsorbed on the nitric acid-reacted surface to the clean surface show some small differences in the infrared spectra of adsorbed water on these two surfaces (Figure 7). The difference spectra show a positive peak at 3511 cm^{-1} and 3699 cm^{-1} that increase in intensity as %RH increases. This feature may be associated with molecular nitric acid in the water layer

(34) Knözinger, H. *Adv. Catal.* **1976**, *25*, 184.
(35) Johnson, M. A.; Stefanovich, E. V.; Truong, T. N.; Günster, J.; Goodman, D. W. *J. Phys. Chem. B* **1999**, *103*, 3391.
(36) Henderson, M. A. *Surf. Sci. Rep.* **2002**, *46*, 1.
(37) Miranda, P. B.; Xu, L.; Shen, Y. R.; Salmeron, M. *Phys. Rev. Lett.* **1998**, *81*, 5876.
(38) Al-Abadleh, H. A.; Grassian, V. H. Submitted for publication in *J. Phys. Chem. B*.

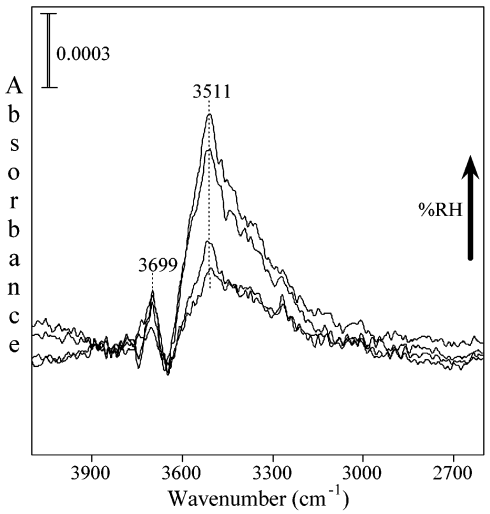

Figure 7. Difference FT-IR spectra of adsorbed water spectrum after reaction of nitric acid minus the adsorbed water spectrum before reaction with nitric acid at 1.4, 2.8, 5.2, and 6.4% RH.

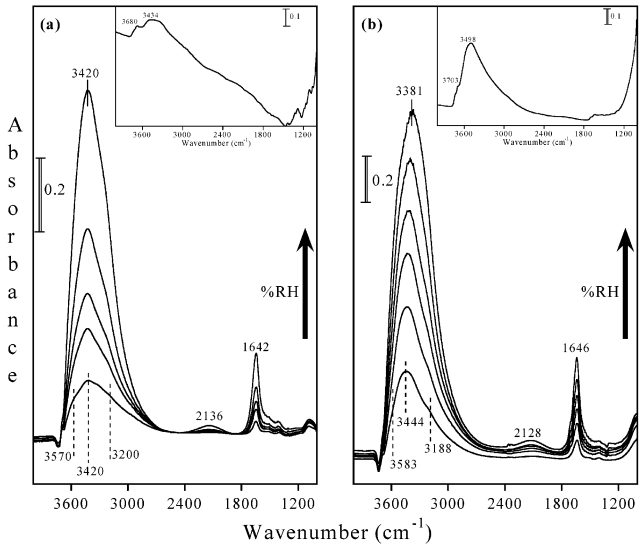

Figure 8. Transmission FT-IR spectra for water adsorption on alumina powder at 296 K as a function of relative humidity: **(**a**)** α-Al_2O_3 (11, 45, 66, 82, 94%), and **(b)** γ-Al_2O_3 (9.5, 33, 66, 85, 93, 99%). Spectra were recorded in the presence of gas-phase water and then gas-phase absorptions were subtracted out. % RH = $P/P_o \times 100$, $P_o = 21.08$ Torr at 296 K. The insets show the spectrum of (a) α-Al_2O_3, (b) γ-Al_2O_3 powders prior to water adsorption.

or a different hydrogen bonding configuration of water molecules at the interface.

4. FT-IR Spectra of Water Adsorbed on α-Al_2O_3 and γ-Al_2O_3 Powders at 296 K. To compare the single-crystal data to the powder data, spectra of water adsorption on α- and γ-Al_2O_3 powders at 296 K as a function of water vapor pressure were recorded and are shown in Figure 8. Infrared spectra of the powdered alumina surfaces were recorded after evacuation overnight and before introducing water. The spectra of these clean surfaces showed absorptions associated with surface hydroxyl groups (insets shown in Figure 8). The spectra of the alumina surfaces in the presence of water vapor were then recorded and referenced to the surface prior to water adsorption. As was done with the single-crystal data, gas-phase water absorptions were subtracted out from the spectra shown in Figure 8. For α-Al_2O_3, the OH stretching absorption bands were centered around 3420 cm^{-1} with obvious shoulders near 3200 cm^{-1} and around 3570 cm^{-1} at the lowest coverage. At higher coverages, there is no significant frequency shift of the OH stretch. The adsorbed H_2O bending mode centered around 1642 cm^{-1} compares fairly well with the bending mode in bulk water. Similarly for γ-Al_2O_3, the spectra at low coverages show an absorption maximum of 3444 cm^{-1} in the OH stretching region with shoulders at 3188 and 3583 cm^{-1}. At high water coverages, the maximum absorption is red-shifted to 3381 cm^{-1}. For water adsorption on γ-Al_2O_3, the frequency of the bending mode vibration is 1646 cm^{-1}. It can be also observed for both alumina samples that there is a negative feature around 3734 cm^{-1}. This feature is associated with the loss of isolated OH groups on the surface due to hydrogen bonding to adsorbed water molecules. Although the spectra shown in Figure 8 shows similar band assignment with bulk liquid water, the OH band frequency is higher than that of liquid water and very close to the OH band frequency at water adsorbed on α-Al_2O_3(0001). The similarities in the OH frequencies and shape of the OH absorptions between the powder and single crystal FT-IR data suggest that water adsorption on Al_2O_3 surfaces takes place in an ordered fashion and produces thin films of water that are more ordered than bulk water.

The association band which is a combination of the bending (δ), frustrated rotation (liberation) (ν_L), and hindered translation (ν_T), modes is observed at 2136 cm^{-1} for α-Al_2O_3 and near 2128 cm^{-1} for γ-Al_2O_3. Those values are close to the combination band of liquid water. The combination band is not observed on single-crystal surfaces and is most likely due to water in the pores of the powdered samples, thus underscoring the difficulty in studies of powdered samples where both adsorption and pore filling may occur simultaneously.

Conclusions

In this study, the adsorption of water at 296 K in the RH range of 1−95% on α-Al_2O_3(0001) and on α- and γ-Al_2O_3 powders has been investigated using FT-IR spectroscopy. The single-crystal data provide detailed information at the molecular level that is more difficult to obtain from powder samples. It was inferred from our study that water adsorbs on the surfaces of alumina in an ordered fashion up to 70% and low coverage data are consistent with the formation of a stable hydroxide hydrogen-bonded to molecular water. This study shows the ability of alumina to potentially act as heterogeneous ice nuclei because the first few layers are ordered even at room temperature.

Acknowledgment. The authors thank Dr. Angela Goodman for providing the infrared data for water adsorption on γ-Al_2O_3 powder. The authors gratefully acknowledge the National Science Foundation for support of this work (CHE-9988434).

LA026208A